LETTERS

Solid-state quantum memory using the ^{31}P nuclear spin

John J. L. Morton[1,2], Alexei M. Tyryshkin[3], Richard M. Brown[1], Shyam Shankar[3], Brendon W. Lovett[1], Arzhang Ardavan[2], Thomas Schenkel[4], Eugene E. Haller[4,5], Joel W. Ager[4] & S. A. Lyon[3]

The transfer of information between different physical forms—for example processing entities and memory—is a central theme in communication and computation. This is crucial in quantum computation[1], where great effort[2] must be taken to protect the integrity of a fragile quantum bit (qubit). However, transfer of quantum information is particularly challenging, as the process must remain coherent at all times to preserve the quantum nature of the information[3]. Here we demonstrate the coherent transfer of a superposition state in an electron-spin 'processing' qubit to a nuclear-spin 'memory' qubit, using a combination of microwave and radio-frequency pulses applied to ^{31}P donors in an isotopically pure ^{28}Si crystal[4,5]. The state is left in the nuclear spin on a timescale that is long compared with the electron decoherence time, and is then coherently transferred back to the electron spin, thus demonstrating the ^{31}P nuclear spin as a solid-state quantum memory. The overall store–readout fidelity is about 90 per cent, with the loss attributed to imperfect rotations, and can be improved through the use of composite pulses[6]. The coherence lifetime of the quantum memory element at 5.5 K exceeds 1 s.

Classically, transfer of information can include a copying step, facilitating the identification and correction of errors. However, the no-cloning theorem limits the ability to faithfully copy quantum states across different degrees of freedom[7]; thus, error correction becomes more challenging for quantum information than for classical, and the transfer of information must take place directly. Experimental demonstrations of such transfer include moving a trapped ion qubit in and out of a decoherence-free subspace for storage purposes[8] and optical measurements of nitrogen-vacancy centres in diamond[9].

Nuclear spins are known to benefit from coherence times long in comparison with those of electron spins, but are slow to manipulate and suffer from weak thermal polarization. A powerful model for quantum computation is thus one in which electron spins are used for processing and readout and nuclear spins are used for storage. The storage element can be a single, well-defined nuclear spin, or perhaps a bath of nearby nuclear spins[10]. ^{31}P donors in silicon provide an ideal combination of long-lived spin-1/2 electron[11] and nuclear spins[12], with the additional advantage of integration with existing technologies[4] and the possibility of single-spin detection by electrical measurement[13–15]. Direct measurement of the ^{31}P nuclear spin by NMR has only been possible at very high doping levels (for example near the metal–insulator transition[16]). Instead, electron–nuclear double resonance can be used to excite both the electron and nuclear spins associated with the donor site, and measure the nuclear spin by means of the electron[17]. This was recently used to measure the nuclear spin-lattice relaxation time, T_{1n}, which was

found to follow the electron relaxation time, T_{1e}, over the range 6–12 K with the relationship $T_{1n} \approx 250 T_{1e}$ (refs 5, 12). The suitability of the nuclear spin as a quantum memory element depends more critically on the nuclear coherence time, T_{2n}, the measurement of which has now been made possible through the storage procedure described here: varying the storage time and observing the amplitude of the recovered electron coherence.

Figure 1b shows the coherence transfer scheme used for the write process from a processing qubit represented by an electron-spin degree of freedom to a memory qubit residing in a nuclear-spin degree of freedom. Each π pulse is equivalent to a controlled-NOT gate[18] (with some additional phase that can be ignored) such that the pair of π pulses constitute a SWAP gate.

The scheme assumes that all pulses are on-resonance and have sufficient bandwidth to completely excite an individual transition. A read operation is performed by applying the reverse sequence, to bring the coherent state back to the electron-spin qubit. Although the phase relationship between the microwave and radio-frequency
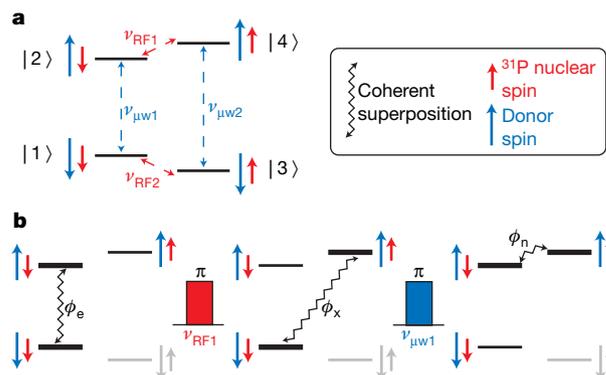

Figure 1 | The level structure of the coupled electron and nuclear spins and scheme for the transfer of a logical qubit within the two physical spin qubits. a, The four-level system may be manipulated by resonant microwave ($v_{μw1}$, $v_{μw2}$) and radio-frequency (v_{RF1}, v_{RF2}) radiation. In our experiments, the logical electron-spin 'processing' qubit is represented by states $|1\rangle$ and $|2\rangle$, whose state can be transferred to a nuclear-spin 'memory' qubit represented by states $|2\rangle$ and $|4\rangle$. State $|3\rangle$ is never addressed at any point and can be ignored. **b**, An electron-spin coherence ϕ_e between states $|1\rangle$ and $|2\rangle$ is transferred to the nuclear-spin qubit by a radio-frequency π pulse followed by a microwave π pulse. Both pulses must fully excite the transition, and be short in comparison with the electron and nuclear coherence times. The reverse process is used to transfer the nuclear coherence ϕ_n back to the electron. The intermediate state ϕ_x is a double quantum coherence representing an entangled electron-nuclear spin state.

[1]Department of Materials, Oxford University, Oxford OX1 3PH, UK. [2]CAESR, Clarendon Laboratory, Department of Physics, Oxford University, Oxford OX1 3PU, UK. [3]Department of Electrical Engineering, Princeton University, Princeton, New Jersey 08544, USA. [4]Lawrence Berkeley National Laboratory, 1 Cyclotron Road, Berkeley, California 94720, USA. [5]Department of Materials Science and Engineering, University of California, Berkeley, California 94720, USA.

pulses must be constant throughout this process, any phase difference is cancelled out over the course of the write–read process. In practice, this means that the microwave and radio-frequency sources need not be phase locked, but must have high phase stability. This is illustrated in calculations following the evolution of the density matrix, provided in the Supplementary Information.

Although the electron-spin qubit can be prepared in a state of high purity using experimentally accessible magnetic fields and temperatures, the small nuclear Zeeman energy results in the nuclear spin being initially in a highly mixed thermal state. However, for the purposes of this quantum memory scheme it is not necessary to perform any pre-cooling of the nuclear-spin resource.

This model is sufficient given a single electron–nuclear spin pair or a homogenous ensemble. However, in the experiment described here we must consider the effects of inhomogeneous broadening across the ensemble of spins being manipulated. The effect of inhomogeneous broadening is to leave some electron spins detuned from the applied microwave radiation, by δ_e, and some nuclear spins detuned from the applied radio-frequency radiation, by δ_n. In a suitable rotating reference frame, electron- and nuclear-spin coherences will thus acquire additional phases at the respective rates δ_e and δ_n, whereas double quantum coherences will acquire a phase at a rate $\delta_e + \delta_n$. Hence, inhomogeneous broadening requires the application of carefully placed refocusing pulses to bring all spin packets into focus at key points during the transfer process. In the experiment described here, $\pi/\delta_e \approx 2\,\mu s$ and $\pi/\delta_n \approx 100\,\mu s$.

Figure 2 shows the practical implementation of a protocol that generates a coherent electron-spin state, stores it in a state of the nuclear spin for some time, and then returns it to the electron state for readout again. The coherence is first generated by a microwave $\pi/2$ pulse of a chosen phase ϕ, representing our bit of quantum information. A free induction decay (that is, the reversible dephasing of the ensemble) follows this pulse. We apply a refocusing microwave
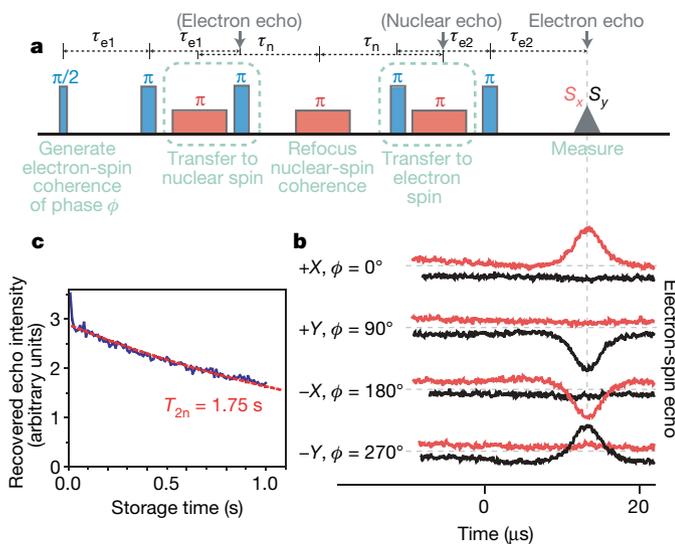
π pulse at time τ_e to initiate a revival in the electron-spin coherence. The subsequent radio-frequency π pulse transfers the coherence from the electron to a double quantum coherence of entangled electron–nuclear spin states. During this period, the phase $\delta_e\tau_e$, acquired before application of the microwave refocusing pulse, continues to reverse in such a way that when the final step of the transfer, a microwave π pulse, is applied, the effect of the inhomogeneous electron-spin packets has been completely refocused. The quantum information that was generated by the first microwave $\pi/2$ pulse now resides entirely in the state of the nucleus.

This information may be stored in the nuclear state for some extended period, so the effects of inhomogeneities on the phase of the nuclear state become appreciable and a preparatory radio-frequency refocusing pulse must be applied before the information can be recovered. During the nuclear-spin echo, the coherence is transferred back to the electron state with a microwave π pulse followed by a radio-frequency π pulse. We apply one further microwave π pulse to stimulate an electron-spin echo representing the readout event. Figure 2b shows the real (red) and imaginary (black) parts of this echo for different initial phases ϕ, demonstrating that the encoded phase is recovered through the storage–recovery process, as required for an effective quantum memory element.

The storage time is limited only by the nuclear decoherence time, T_{2n}, which is in turn limited to $2T_{1e}$ when there is a significant hyperfine interaction ($A \gg 1/T_{1e}$) between the electron and nuclear spins and in the limit where the thermal energy exceeds the magnetic field splitting ($k_B T \gg g\mu_B B$; see Supplementary Information); T_{1e} becomes very long (for example hours) at low temperatures[17]. A direct measurement of T_{2n} in anything other than highly doped Si:P has been impossible by traditional NMR means, but our write–read procedure provides a method of performing this measurement by increasing the storage time, T_{store}, and observing the resulting decay in the recovered electron coherence. The T_{2n} obtained in this way follows $2T_{1e}$ approximately over the range 9–12 K as expected, though at lower temperatures an additional nuclear decoherence mechanism appears to have a role, yielding a limit of about 65 ms for T_{2n}. A leading candidate for this additional process is slowly fluctuating fields, the effect of which may be mitigated by dynamically decoupling the system[19,20]. By applying a Carr–Purcell–Meiboom–Gill decoupling sequence at a 1-kHz repetition rate to the nuclear spin during the storage period, we were able to obtain much longer decoherence times than for a simple Hahn echo measurement, rising to 1.75 s at 5.5 K, as shown in Fig. 2c.

Under optimized conditions, the electron-spin decoherence time, T_{2e}, is limited only by magnetic dipole–dipole interactions, and values between 4 and 6.5 ms have been measured in the samples used here, varying according to the donor-spin concentration[11]. Using the nuclear degree of freedom, we have achieved storage times several orders of magnitude longer than T_{2e}.

The removal, or substantial detuning, of any of the radio-frequency pulses in the sequence destroys the recovered echo, confirming the importance of the transfer to the nuclear spin and providing evidence that the stored quantum information does reside in the nuclear state. For a more direct proof, we require a tool permitting inspection of the state of the nuclear spin during the storage period. We therefore applied a sequence to probe (destructively) the nuclear coherence through the electron state, as shown in Fig. 3a. The early part of the sequence is as described above: an electron-spin coherence is stored in the state of the nucleus. When we decide to observe the state of the nucleus, we apply a radio-frequency $\pi/2$ pulse to convert the nuclear coherence into a nuclear polarization (in the spirit of a Ramsey fringe experiment). A short electron-spin echo sequence, selective in one nuclear subspace, then reveals the population of the nuclear level.

This sequence can be performed at any time; Fig. 3b shows the result of observing the state of the nucleus at a range of times for different starting phases ϕ, revealing the nuclear-spin echo following

Figure 2 | Coherent storage of an electron-spin state in a nuclear-spin state, using a ^{31}P-doped ^{28}Si-enriched silicon single crystal. a, The general sequence for the storage and revival of the electron-spin state comprises microwave and RF pulses applied at certain times, defined by τ_{e1}, τ_{e2} and τ_n. **b**, An electron-spin coherence is stored in the nuclear spin for $2\tau_n \approx 50$ ms, at 7.2 K. Real (red) and imaginary (black) parts of the recovered electron-spin echo are shown for different initial phases ϕ. The echo is of comparable intensity to that obtained at the beginning of the sequence, even though the electron-spin coherence time, T_{2e}, is about 5 ms here. The lifetime of the stored state is limited instead by the nuclear decoherence time, T_{2n}, which can be measured directly by varying τ_n. **c**, The recovered echo intensity was measured as a function of the storage time at 5.5 K while a dynamic (Carr–Purcell–Meiboom–Gill) decoupling sequence was applied to the nuclear spin, yielding a T_{2n} exceeding 1 s.
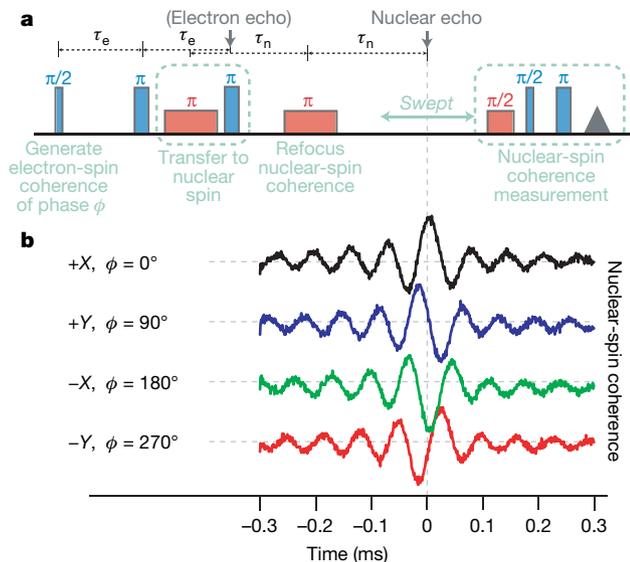
Figure 3 | Observing the nuclear-spin coherence during the storage process. a, The phase of the initial electron superposition state is determined by the phase of initial microwave $\pi/2$ excitation pulse, which we can control. This state is then transferred to the nuclear spin using the scheme outlined in Fig. 1. The nuclear-spin coherence is read using a process similar to a Ramsey fringe measurement: a radio-frequency $\pi/2$ pulse converts nuclear coherence to nuclear polarization, which is then detected by means of an electron spin echo measurement selective of one nuclear-spin state. **b**, The correlation of the phase of the nuclear-spin echo and the phase of the original electron-spin superposition confirms the coherent nature of the transfer from electron to nuclear spin.

the radio-frequency refocusing pulse. The centre of the radio frequency was intentionally moved off-resonance to produce oscillations in the nuclear echo and, hence, aid the identification of the phase of the nuclear coherence. The fact that the phase of the nuclear-spin echo follows the phase of the original microwave $\pi/2$ pulse confirms that the information transfer process has remained coherent. In contrast to other nuclear-spin echoes observed by means of electron–nuclear double resonance[21,22], in which an electron-spin polarization is used to create a nuclear-spin polarization and then a nuclear coherence, this echo represents a coherent state of the electron that has been directly transferred to the nuclear spin.

To demonstrate the generality of the storage sequence described here, we applied it to a wider set of initial states, in particular the $\pm X$, $\pm Y$, $\pm Z$ (spin component direction) and identity basis states, and performed density matrix tomography by comparing the original states with those recovered after the write–read process (see Supplementary Information for full details). The results are summarized in Fig. 4 and show fidelities of approximately 0.90, where the fidelity between the initial (pseudo)pure state, ρ_0, and the recovered state, ρ_1, is defined as $F = \langle\psi|\rho_1|\psi\rangle$, where $\rho_0 = |\psi\rangle\langle\psi|$. We attribute the reduced fidelity to a $\sim$5% error in each of the seven microwave and radio-frequency pulses applied over the course of the sequence, which is entirely consistent with previous measurements of pulse fidelities[23]. Such errors are mostly systematic and may be corrected through the application of composite pulses, as previously demonstrated in both electron paramagnetic resonance (EPR) and NMR[6,24]. By replacing some of the microwave pulses with BB1 composite pulses, we were able to improve the overall fidelity to approximately 0.97, and further improvements are to be expected with greater control of the radio-frequency pulse phases.

As the experimental challenges of quantum information processing have become better understood, the importance of hybrid quantum systems in models of quantum information has emerged[25–27]. The approach described here demonstrates the advantages of such hierarchical models and has a broad applicability in
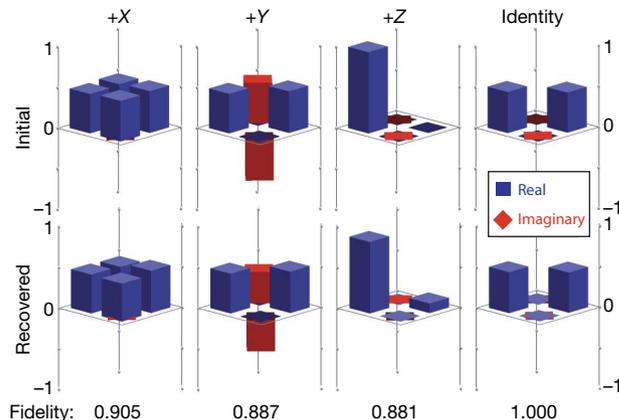

Figure 4 | Density matrix tomography for original and recovered states. Pseudopure states $+X$, $+Y$ and $+Z$ and the identity were prepared in the electron-spin qubit and measured (first row, initial). These states were then stored in the nuclear-spin degree of freedom and then returned to the electron spin and measured (second row, recovered). Tomography was performed by measuring the qubit in the $(\sigma_x, \sigma_y, \sigma_z)$ basis. The fidelity of the quantum memory was obtained by comparing the initial and recovered density matrices.

systems where there is a substantial asymmetry in relaxation times. Storage can be driven globally, as shown here, or locally, using EPR gates[28] or Stark tuning[4]. Furthermore, our protocol for faithfully transferring a coherent electron-spin state to the nuclear spin offers a route to projective measurements of the qubit state through proposed spectrally sensitive single-spin-detection methodologies such as EPR detected either using scanning tunnelling microscopy or electrically[29].

METHODS SUMMARY

Si:P consists of an electron spin, $S = 1/2$ ($g = 1.9987$), coupled to the nuclear spin, $I = 1/2$, of ^{31}P through a hyperfine coupling $A = 117$ MHz (ref. 17), and is described by an isotropic spin Hamiltonian $H_0 = \omega_e S_z - \omega_I I_z + ASI$ (in angular frequency units), where, respectively, S and I are the electron and nuclear spin tensors, $\omega_e = g\beta B_0/\hbar$ and $\omega_I = g_I\beta_n B_0/\hbar$ are the electron and nuclear Zeeman frequencies, g and g_I are the electron and nuclear g-factors, β and β_n are the Bohr and nuclear magnetons, $\hbar$ is Planck's constant divided by 2π and B_0 is the magnetic field applied along z axis in the laboratory frame. The X-band EPR signal comprises two lines (one for each nuclear-spin projection $M_I = \pm 1/2$). Our experiments were performed on the high-field line of the EPR doublet corresponding to $M_I = -1/2$.

Single-crystal samples were used, as epilayers of ^{28}Si have a biaxial residual stress that broadens the ^{31}P electron–nuclear double resonance line and makes it difficult to fully excite. ^{28}Si-enriched single crystals with a residual ^{29}Si concentration of 800 p.p.m. were produced by decomposing isotopically enriched silane (SiH$_4$) in a recirculating reactor to produce poly-Si rods, followed by floating-zone crystallization[30]. To reduce spin–spin coupling effects, the P concentration was reduced from an initial value of near 1×10^{15} cm^{-3} to 2×10^{14}–5×10^{14} cm^{-3} by five passes of zone refining followed by floating-zone crystallization.

Pulsed EPR experiments were performed using an X-band (9–10 GHz) Bruker EPR spectrometer (Elexsys 580) equipped with a low-temperature helium-flow cryostat (Oxford CF935). An Amplifier Research 20W solid-state continuous-wave amplifier was used, with $\pi/2$ and π pulses of 80 and 160 ns, respectively. Radio-frequency pulses of 20 µs were used for π rotations of the ^{31}P nuclear spins. During Carr–Purcell–Meiboom–Gill decoupling, up to 1,000 refocusing pulses were applied during a single sequence.

1. Deutsch, D. Quantum theory, the Church-Turing principle and the universal quantum computer. *Phil. Trans. R. Soc. Lond. A* **400**, 97–117 (1985).
2. Steane, A. M. Efficient fault-tolerant quantum computing. *Nature* **399**, 124–126 (1999).
3. Julsgaard, B., Sherson, J., Cirac, J. I., Fiuráek, J. & Polzik, E. S. Experimental demonstration of quantum memory for light. *Nature* **432**, 482–486 (2004).
4. Kane, B. E. A silicon-based nuclear spin quantum computer. *Nature* **393**, 133–137 (1998).

1087

5. Tyryshkin, A. M. et al. Coherence of spin qubits in silicon. J. Phys. Condens. Matter 18, S783–S794 (2006).

6. Morton, J. J. L. et al. High fidelity single qubit operations using pulsed electron paramagnetic resonance. Phys. Rev. Lett. 95, 200501 (2005).

7. Wootters, W. K. & Zurek, W. H. A single quantum cannot be cloned. Nature 299, 802–803 (1982).

8. Kielpinski, D. et al. A decoherence-free quantum memory using trapped ions. Science 291, 1013–1015 (2001).

9. Dutt, M. V. G. et al. Quantum register based on individual electronic and nuclear spin qubits in diamond. Science 316, 1312–1316 (2007).

10. Dobrovitski, V. V., Taylor, J. M. & Lukin, M. D. Long-lived memory for electronic spin in a quantum dot: Numerical analysis. Phys. Rev. B 73, 245318 (2006).

11. Tyryshkin, A. M., Lyon, S. A., Astashkin, A. V. & Raitsimring, A. M. Electron spin relaxation times of phosphorus donors in silicon. Phys. Rev. B 68, 193207 (2003).

12. Tyryshkin, A. M., Morton, J. J. L., Ardavan, A. & Lyon, S. A. Davies electron-nuclear double resonance revisited: Enhanced sensitivity and nuclear spin relaxation. J. Chem. Phys. 124, 234508 (2006).

13. Stegner, A. R. et al. Electrical detection of coherent ^{31}P spin quantum states. Nature Phys. 2, 835–838 (2006).

14. McCamey, D. R. et al. Electrically detected magnetic resonance in ion-implanted Si:P nanostructures. Appl. Phys. Lett. 89, 182115 (2006).

15. Lo, C. C. et al. Spin-dependent scattering off neutral antimony donors in ^{28}Si field-effect transistors. Appl. Phys. Lett. 91, 242106 (2007); Appl. Phys. Lett. 92, 109908 (2008).

16. Hirsch, M. J. & Holcomb, D. F. NMR study of Si:As and Si:P near the metal-insulator transition. Phys. Rev. B 33, 2520–2529 (1986).

17. Feher, G. Electron spin resonance experiments on donors in silicon I: Electronic structure of donors by the electron nuclear double resonance technique. Phys. Rev. 114, 1219–1244 (1959).

18. Mehring, M., Mende, J. & Scherer, W. Entanglement between an electron and a nuclear spin 1/2. Phys. Rev. Lett. 90, 153001 (2003).

19. Viola, L. & Lloyd, S. Dynamical suppression of decoherence in two-state quantum systems. Phys. Rev. A 58, 2733–2744 (1998).

20. Morton, J. J. L. et al. Bang-bang control of fullerene qubits using ultra-fast phase gates. Nature Phys. 2, 40–43 (2006).

21. Höfer, P., Grupp, A. & Mehring, M. High-resolution time-domain electron-nuclear-sublevel spectroscopy by pulsed coherence transfer. Phys. Rev. A 33, 3519–3522 (1986).

22. Morton, J. J. L. et al. The N@C60 nuclear spin qubit: Bang-bang decoupling and ultrafast phase gates, Phys. Status Solidi B 243, 3028–3031 (2006).

23. Morton, J. J. L. et al. Measuring errors in single-qubit rotations by pulsed electron paramagnetic resonance. Phys. Rev. A 71, 012332 (2005).

24. Cummins, H. K., Llewellyn, G. & Jones, J. A. Tackling systematic errors in quantum logic gates with composite rotations. Phys. Rev. A 67, 042308 (2003).

25. Taylor, J. M. et al. Fault-tolerant architecture for quantum computation using electrically controlled semiconductor spins. Nature Phys. 1, 177–183 (2005).

26. Thaker, D. D., Metodi, T. S., Cross, A. W., Chuang, I. L. & Chong, F. T. in ISCA '06 378–390 (Proc. 33rd Internat. Symp. Computer Architecture, IEEE, 2006).

27. Rabl, P. et al. Hybrid quantum processors: Molecular ensembles as quantum memory for solid state circuits. Phys. Rev. Lett. 97, 033003 (2006).

28. Nowack, K. C., Koppens, F. H. L., Nazarov, Y. V. & Vandersypen, L. M. K. Coherent control of a single electron spin with electric fields. Science 318, 1430–1433 (2007).

29. Sarovar, M., Young, K. C., Schenkel, T. & Whaley, K. B. Quantum non-demolition measurements of single spins in semiconductors. Preprint at ⟨http://arxiv.org/abs/0711.2343v1⟩ (2007).

30. Ager, J. W. et al. High-purity, isotopically enriched bulk silicon. J. Electrochem. Soc. 152, G448–G451 (2005).